Instrumentation for Very High Energy Gamma-Ray Astronomy

M.F. Cawley
Physics Department,
St. Patrick's College,
Maynooth,
County Kildare, IRELAND.

and

T.C. Weekes
Fred Lawrence Whipple Observatory,
Harvard-Smithsonian Center for Astrophysics,
P.O. Box 97,
Amado,
AZ 85645-0097, U.S.A.

(Received 24 October 1994; accepted 10 February 1995)

Abstract. Considerable progress has been made in the last half-decade in the field of very high energy (VHE) gamma-ray astronomy (photons with energies between 10^{11} and 10^{13}eV). The high background level due to the isotropic cosmic ray flux which has bedevilled the field since its inception in the early 1960's can now be reduced to such a degree that significant gamma-ray signals from several sources become visible within a few hours of observation. The instrumentation and methodologies which have made this possible are reviewed. A brief historical introduction is followed by a summary of the salient properties of the atmospheric Cherenkov flash associated with VHE gamma-ray events. The major components of a VHE gamma-ray astronomy telescope are then reviewed. This is followed by a discussion of the different methodologies currently being used to discriminate against the cosmic ray background. Properties of several specific installations are then summarized, and possible future developments in VHE instrumentation are briefly discussed.

Key words: Gamma-ray Astronomy, Atmospheric Cherenkov Technique

1 The Atmospheric Cherenkov Technique

1.1 Introduction

Gamma-ray astronomy may be divided into several energy regions, which are characterised by distinct experimental methods. As the Earth's atmosphere is opaque to all gamma radiation, direct detection requires that the detectors be borne aloft by balloons or satellites; the small collection areas result in an upper energy limit defined by the energy where fluxes fall below 1 photon per square meter per week.

Above 10^{11}eV, gamma radiation from celestial sources may be detected indirectly via byproducts of the electromagnetic cascade initiated by such photons upon entry into the atmosphere. Between 10^{11} and 10^{13}eV — the 'VHE' energy region — few of the secondary particles in such cascades reach ground level, and indirect detection of the shower relies on the Cherenkov light generated by the charged secondaries (mainly electrons and positrons) before their energy falls below the Cherenkov threshold (21MeV at sea level). This 'atmospheric Cherenkov technique' (ACT) is the principal method available at present in VHE gamma-ray astronomy.

Experimental Astronomy **6**: 7–42, 1995.

Above 10^{13}eV, it is possible to detect the secondary particles in the cascade at high mountain altitudes; above 10^{15}eV, it becomes possible to detect the cascade particles at sea level. Gamma-ray astronomy above 10^{13}eV (the ultra high energy, or 'UHE' region) can therefore be carried out using large arrays of particle detectors.

One important feature distinguishes the methods applied in the VHE and UHE energy regions: the field of view of VHE gamma-ray astronomy instruments is usually relatively small, making all-sky surveys problematic. In simple detector systems which use a single photomultiplier tube (PMT) at the focus of each light collector, the field of view is matched to the angular extent of the Cherenkov flash, which is of order 1°, in order to optimize the signal to noise ratio (see section 1.3). In imaging systems which use clusters of PMT's in the focal plane, the total field of view increases to typically 3° to 4°, but is still limited by the nature of the optical systems and by the expense of increasing the number of PMT's. In addition, the nature of the technique imposes severe restrictions on observing time due to the requirement of clear, dark, moonless skies. Such restrictions do not apply in the UHE energy region, where particle detectors can continually view between 1 and 2 steradians of sky (in typical systems, all events out to zenith angles of between 40° and 50° are accepted). All-sky surveys are therefore possible at these energies. Fluxes, however, are extremely low in the UHE energy region, and to date no gamma-ray sources have been confirmed at high levels of statistical significance.

In this review, we concentrate exclusively on the VHE energy region, which utilizes the atmospheric Cherenkov technique. Following a brief historical introduction, we summarise the main characteristics of the Cherenkov light flash which in turn determine the nature of the instrumentation used in this area. There follows in section 2 a general review of this instrumentation, initially without reference to any specific system. Section 3 outlines some of the methods of telescope calibration. In section 4 we discuss the main experimental methods or 'philosophies of approach' which are currently being tried or planned in the VHE region. In section 5 we briefly review several existing experiments and in section 6 some planned VHE installations.

1.2 Historical Background

The ACT was first used in a systematic manner to search for point VHE gamma-ray sources in the early 1960's. An array of 12 searchlight mirrors, each of aperture 1.5m, was operated in parallel at a site in the Crimea by a group from the Lebedev Institute (Chudakov *et al.* 1965). The energy threshold of the telescope was 4 TeV and the flux sensitivity was $5 \times 10^{-11} photons\ cm^{-2} s^{-1}$. No statistically significant fluxes were detected from a catalog of source candidates which included the Crab Nebula, Cassiopeia A and Cygnus A. Similar systems were deployed elsewhere during the 1960's; all of these 'first generation' detectors used relatively small mirrors operating singly or in coincidence. They searched for excess count rates in the direction of suspected VHE sources, but no means were available for

rejecting triggers generated by the much more abundant charged cosmic rays. It became evident as work on such systems progressed that some means of rejecting a significant proportion of the background was required.

Ambitious second generation detectors were begun in the early 1980's. Two main approaches were tried: using a distributed array of detectors to perform fast timing on the Cherenkov shower front, thereby improving the angular resolution, and recording images of the Cherenkov flash with a view to exploiting differences in images of gamma-ray initiated and cosmic-ray initiated showers. The first unequivocal detection of a VHE gamma-ray source was achieved via the imaging technique; a 9σ effect was observed from the Crab Nebula using a 37-PMT array on the Whipple Observatory 10m reflector (Weekes *et al.* 1989) followed by a 20σ effect using a 109-PMT array (Vacanti *et al.* 1991). The Crab Nebula is now established as a steady VHE emitter ($7 \times 10^{-11} photons\, cm^{-2} s^{-1}$ for E > 400 GeV) and is routinely used as a standard candle source to calibrate new detectors and test the efficacy of new approaches. (For example, the Crab Nebula has also been detected at high levels of statistical significance by the THEMISTOCLE collaboration who accurately measure the time of arrival of the Cherenkov light front using an array of detectors; Baillon *et al.* 1993a.) Other sources have also been detected using the imaging technique, including the gamma-ray pulsar PSR1706-44 (Ogio *et al.* 1993) and the distant galaxy Markarian 421 (Punch *et al.* 1992). In the last decade of the 20th century, VHE gamma-ray astronomy has finally come of age.

1.3 Detection of Cherenkov light from Air Showers

The Cherenkov light flash from an air shower can be detected against the night-sky light by virtue of its duration and spectrum. The typical night-sky light flux is $10^{12} photons\, m^{-2} s^{-1} sr^{-1}$ between 3300Å and 4500Å. This can vary by a large factor depending on site quality and atmospheric conditions. A typical Cherenkov flash lasts for about 5ns and yields about $50 photons m^{-2}$ within 100m of the shower axis for a 1TeV gamma-ray primary. If the field of view of a detector is matched to the angular extent of the Cherenkov flash, which is of order 1°, the night-sky light detected in 5ns will be of order 1 to 2 photons per square meter. Thus the Cherenkov flash may readily be detected above the fluctuations in the night-sky light, even at a non-optimal site. As the Cherenkov spectrum peaks in the blue to near UV, whereas the sky light increases towards the red end of the spectrum, the PMT spectral responses may be chosen to match the Cherenkov spectrum.

The night-sky light background is the key factor determining the energy threshold of ACT systems. For a simple 'first generation' system with a single PMT at the focus of each collecting element, the sky noise fluctuations are given by

$$N = \sqrt{\int_{\lambda_1}^{\lambda_2} B(\lambda)\epsilon(\lambda)\Omega t d\, d\lambda} \qquad (1)$$

where $B(\lambda)$ is the background light flux as a function of wavelength λ, $\epsilon(\lambda)$ is the quantum efficiency, Ω is the solid angle, t is the integration time, d is the mirror

area, and λ_1 and λ_2 are the bounds of the wavelength region over which the system is sensitive. Assuming that the integration time t is equal to or longer than the duration of the Cherenkov flash, the air shower signal is given by

$$S = \int_{\lambda_1}^{\lambda_2} C(\lambda)\epsilon(\lambda)\Omega d\, d\lambda \tag{2}$$

where $C(\lambda)$ is the Cherenkov photon flux ($photons\ m^{-2}sr^{-1}$). In first generation systems Ω is normally chosen to match the characteristic size of the Cherenkov flash, so that the product $C(\lambda)\Omega$ is optimized to collect all the Cherenkov photons hitting the light collector. The signal-to-noise ratio is then

$$S/N = \int_{\lambda_1}^{\lambda_2} C(\lambda)\sqrt{\frac{\epsilon(\lambda)\Omega d}{B(\lambda)t}}\, d\lambda\,. \tag{3}$$

The smallest detectable Cherenkov light pulse is inversely proportional to S/N as is the minimum shower energy threshold; hence

$$E_T \propto \frac{1}{C(\lambda)}\sqrt{\frac{B(\lambda)t}{\epsilon(\lambda)\Omega d}}\,. \tag{4}$$

A more useful parameter is the effective energy threshold, (i.e. mean energy of detected events) — this depends on the source spectrum but is usually within a factor of 2 or 3 of the threshold energy (section 3).

Apart from the threshold energy, the other main parameter used to characterize an atmospheric Cherenkov detector is its minimum flux sensitivity at the effective energy threshold. In this case, the 'background' consists of the isotropic cosmic ray flux, and the noise fluctuation is given by

$$N = \sqrt{k_b E_b^{-1.7} A_b(E_b)\Omega T} \tag{5}$$

whereas the signal flux is given by

$$S = k_g E_g^{-G} A_g(E_g) T \tag{6}$$

where E_g is the gamma-ray energy threshold, E_b the background cosmic-ray energy threshold, G the integral power law exponent of the gamma-ray source, $A_g(E_g)$ the collection area for gamma rays, $A_b(E_b)$ the collection area for background cosmic rays, Ω the detector solid angle, T the observation time, and k_g and k_b are constants characterizing the flux levels of the source and background (Weekes, 1988). The signal-to-noise ratio can be expressed in terms of N_{sig}, the number of standard deviations at which the signal is detected:

$$N_{sig} = \frac{k_g E_g^{-G} A_g(E_g) T^{\frac{1}{2}}}{\sqrt{k_b E_b^{-1.7} A_b(E_b)\Omega}}\,. \tag{7}$$

If we assume that $E_g \propto E_b$ and that A_g and A_b are approximately independent of energy above threshold, then this expression simplifies to

$$N_{sig} \propto \frac{A_g T^{\frac{1}{2}} E^{0.85-G}}{\sqrt{A_b \Omega}} . \tag{8}$$

To maximize N_{sig} (and hence get the best flux sensitivity) we can (1) increase the collection area for gamma rays — this is achieved by operating with a geometric solid angle that exploits the flat lateral distribution in the gamma-ray showers and by using other background discrimination methods that do not reduce the efficiency of gamma-ray detection; (2) increase the observation time (of limited value for transient sources); (3) operate at the energy which gives the maximum N_{sig} (i.e. going to the minimum possible energy threshold for sources where $G > 0.85$; only for sources with very flat energy spectra is it advantageous to operate at high energies); (4) minimize the effective collection area ($A_b\Omega$) for background cosmic rays by using some method of discrimination (section 4).

2 Components of a VHE Gamma-ray Astronomy Telescope

2.1 Light Collectors

Although the light collectors used in the ACT are essentially optical telescopes, their key properties are usually quite different from those used in large astronomical telescopes. The relatively crude structure of the Cherenkov flash (of order 0.1°) makes arc-minute resolution unnecessary. [1] On the other hard, the angular extent of the flash means that the field of view must be at least of order 1°, and considerably more for Cherenkov imaging systems. Some representative light collection arrangements are summarized in table I, and a number of atmospheric Cherenkov telescopes are shown in figure 1. Large mirror collection areas are desirable in order to reduce the threshold energy. The large collection area is typically accomplished using a tessellated approach, with many small spherical or paraboloidal elements on a single mount, focusing to a common focal plane. Some more recent systems have used composite mirrors, i.e. a continuous large surface area composed of several segments.

Plate scale requirements associated with clusters of PMT's typically result in f-numbers (ratio of focal length to diameter) of around 0.7 to 1.0. Appreciably smaller f-numbers are undesirable because of severe abberations. The choice of optimal mirror shape and f-number depend to a large extent on the aims of the particular experiment. If preservation of the timing of the shower front is an overriding consideration (for fast timing purposes, or optimal triggering on low energy events) then a paraboloidal figure is required, and f-numbers of unity or greater

[1] Hillas (1989) has shown using simulations that angular resolution of a few arcminutes may be possible using stereoscopic systems and high resolution detectors such as image intensifiers.

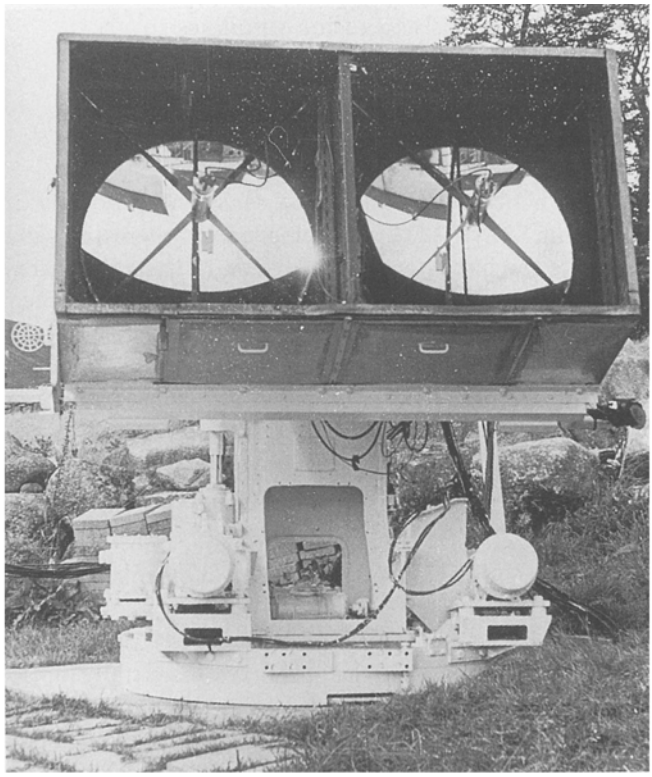

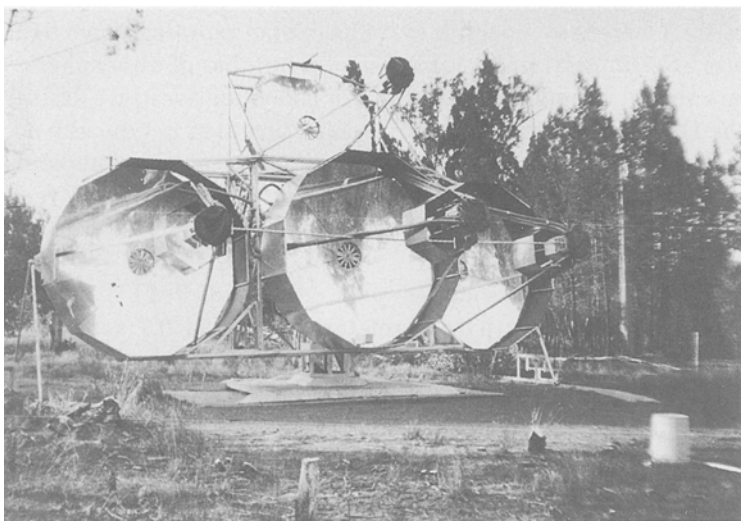

Fig. 1. A number of atmospheric Cherenkov telescopes. Top (this page): searchlight mirrors used at Glencullen, Ireland, in the 1960's; Bottom (this page): the Durham Mark Va detector at Narrabri, Australia; Top (next page): the 10m diameter reflector at Mt. Hopkins, Arizona; Bottom (next page): the 3.8m reflector used in the CANGAROO experiment.

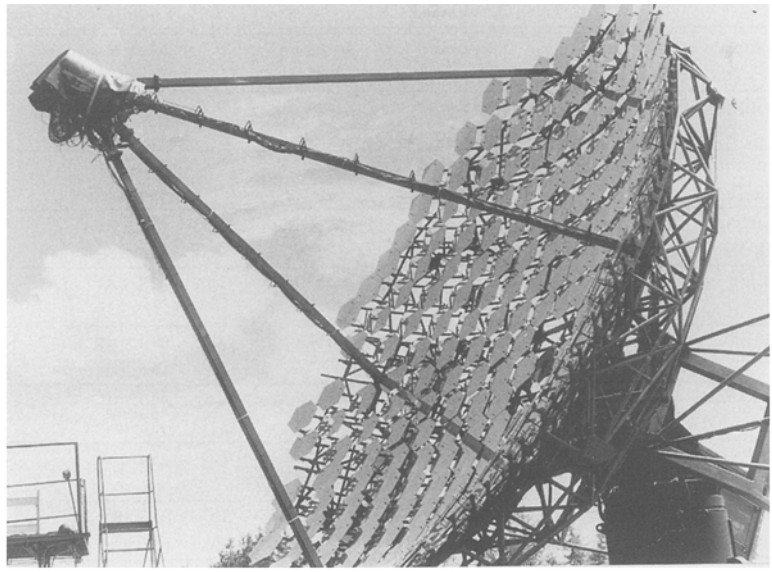

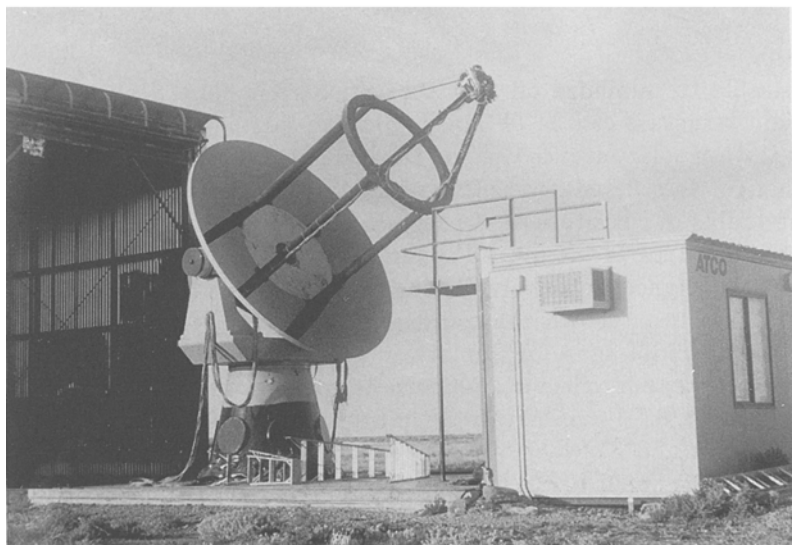
ATCO

TABLE I
Properties of ACT Light Collectors.

Group	Aperture	Single/ Tesselated	Shape	f/	Coating	Spot size (on axis)
Whipple	10m	tesselated 248 segments	spherical	0.7	Al,front anodized	0.13°
Whipple	11m	tesselated 433 segments	parabolic	0.7	Al,back	0.2°
Durham MkIII	4m	tesselated 43 elements	parabolic	0.6	Al,front anodized	0.2°
Durham Mk VI	7m	composite 24 sectors	parabolic	1.0	Al,front anodized	0.125°
CLUE	1.8m	single	parabolic	1.0	Al,front	0.1°
GASP	0.8m	10 elements in parallel	parabolic	1.06	Al,front anodized	
HEGRA	3m	tesselated 18 elements	spherical	1.6	Al,front quartz	0.07°
CANGAROO	3.8m	composite 7 segments	parabolic	1.0	Al,front	0.016°
Nooitge-dacht	1.5m	tesselated 3 elements	spherical	1.0	Al,oxide coating	
CAT	4.8m	tesselated 90 segments	spherical	1.25	Al,front anodized	0.02° (estimated)

are desirable to minimize off-axis abberations. A more compact and mechanically rigid structure can be obtained with the sacrifice of isochronicity using the Davies-Cotton solar furnace design (Davies and Cotton, 1957). In this approach, the spherical tessellated segments are mounted on a spherical frame which has half the radius of curvature of the segments. The focal plane is positioned at the centre of curvature of the overall spherical frame, and the axes of the individual segments are aligned to converge at their centre of curvature. In a study by Lewis (1990), it has been shown that such a design gives better off-axis performance than a paraboloidal figure of similar f-number. This design is used in the Whipple Observatory 10m reflector, and permits good imaging performance despite the relatively fast f/0.7 f-number. A similar design is proposed for the CAT project (Degrange *et al.* 1993), where a slower f-number of f/1.25 will be used to facilitate higher resolution imaging. In general, the trend in recent and proposed systems is to move towards slower (> 1.0) f-numbers in order to achieve quasi-isochronicity accompanied by good off-axis performance for high resolution imaging.

A common manufacturing technique for mirrors used in VHE gamma-ray astronomy is slumping on a machined mould (e.g. Loeffler, 1993). In this method, glass flats of thickness 6mm (typical) are slowly heated to around 600℃ over a

metal or graphite mould (of spherical or paraboloidal figure) until the glass slumps to assume the shape of the mould. Slow cooling removes internal stresses. The front surface (which was not in contact with the mould) is then aluminized and often anodized to give improved durability (Harris *et al.* 1992). Front coating with aluminium typically gives 80% reflectivity or better over a wide range of wavelengths (220-800nm) and permits observations into the UV region.

Other methods of mirror manufacture include fixing polished aluminium sheeting to shaped aluminium honeycomb, and gluing thin glass sheeting (back aluminized) to shaped glass foam (Brazier *et al.* 1989; Weaverdyck, Meyer, and Akerlof, 1991). Such methods lead to much lighter mirror structures. One drawback associated with this type of mirror is that they tend to have small heat capacity and poor thermal grounding to the telescope mount; radiative cooling can lead to problems of condensation and icing.

Apart from the primary light collection surface, a variety of additional optical components are being increasingly employed in VHE telescope systems in an effort to optimise Cherenkov light collection while reducing the effects of non-Cherenkov light contamination. Non-imaging concentrators ('light cones') placed in front of the PMT arrays in the focal plane may be used to partially compensate for the dead space between arrays of circular pixels (Aharonian *et al.* 1991a; Degrange *et al.* 1993). The efficacy of such cones in terms of improving the signal-to-noise for gamma-ray detection has yet to be conclusively demonstrated. The same can be said for the use of filters to remove part of the night-sky background which peaks towards the red end of the spectrum (e.g. Resvanis *et al.* 1988). One ancillary optical technique which should certainly offer some degree of improvement for large light collection systems is the deployment of anti-albedo screens around the primary collecting surface and in the vicinity of the focal plane. Such screening prevents light from reaching the detector array in the focal plane unless it has first been reflected off the primary mirror surface. Light cones have a similar screening effect.

2.2 Light Detectors

The low light level of the Cherenkov flash combined with its short ($< 5ns$) duration and predominance towards the blue end of the visible spectrum makes the photomultiplier tube the most suitable detector. Properties of some representative PMT's used in the atmospheric Cherenkov technique are summarised in table II. The operating conditions of the PMT's in ACT systems are unusual, however, in that they are exposed to high levels of background light from the night sky as a consequence of the large light collection areas. Anode current levels of up to 30μA are typical, approaching the maximum recommended limits. Individual pixels in imaging arrays of PMT's often have to be powered down due to the presence of bright stars in the vicinity of the gamma-ray source. Such severe operating conditions tend to cause ageing of the photocathode, necessitating periodic adjustments (over months to years) of the high voltage settings to compensate for gain losses.

TABLE II
Photomultiplier Tubes used in ACT Systems.

Group	PMT Type	Diameter (mm)	Risetime (ns)	Gain ($\times 10^6$)	Spectral Response	Stages
Durham Mark III	RCA 8575	50	2.6	1.3	300–650nm	12 signal from 11th
Halea-kala	Hamamatsu R-1450	19	1.8	2.0	300–650nm	10
Whipple	Hamamatsu R-1398	28	2.2	2.1	300–650nm	10 replacement: R3082
CAT	Hamamatsu 1635-02	10	0.8	2.2	300–650nm	8
CANGAROO	Hamamatsu R-2248	10 (square)	0.9	1.0	300–650nm	8

In typical systems, negative high voltage is applied to the photocathode of the PMT which allows for monitoring of the anode current, and also allows for the use of feedback to LED's in front of the PMT's which may be used to maintain a constant level of background illumination (servo lamps). Mu-metal magnetic shields are invariably used around the PMT's in ACT systems to prevent changes in gain as a result of changes in orientation relative to the Earth's magnetic field.

The key requirements of a light detector for use in the ACT are:

- fast response (the time scale should be matched to that of the Cherenkov pulse),
- high gain (to avoid the necessity of very high amplifier gain in signal processing, which would introduce additional noise and limit bandwidth),
- good blue to UV efficiency (to match the Cherenkov spectrum, and reduce effects of night-sky light which peaks towards the red),
- low intrinsic noise under high illumination.

The last point is addressed in some detail by Brazier *et al.* (1989). They show that there is considerable variation in noise performance as a function of photocathode illumination for different PMT's operating under similar conditions of gain and anode current. They also found that some tubes exhibited gain instabilities under high photocathode illumination. In this respect, desirable properties of a PMT for use with the ACT are a relatively slow rise in the rate of noise-induced pulses ('noise singles rate') with increased illumination, and a stable gain under constant high levels of illumination.

The move towards higher resolution in Cherenkov imaging systems introduces additional requirements and limitations for detector arrays. The lower limit in

TABLE III
Properties of Multipixel Detectors.

Detector	Speed	Pixel size (typical)	No. of pixels	Gain	Spectral Response
PMT discrete	1ns	> 10mm	1	10^6	200-700nm
PMT multianode	5ns	2.5mm	64 - 96 (typical)	10^6	280-620nm
Image Intensifier	5ns (gated)	0.1mm	10^6	10^7	
UV-gas (CLUE)	2ns	10mm	16 x 16	10^7 (multistage)	190-230nm
Solid State APD	< 1ns	0.4mm	1	10^3 at 150V	200-1100nm
Solid State Si photodyode	4ns	25mm	1	10^3 at 10kV	

physical size of about 1cm for discrete PMT's imposes a limiting resolution of order 0.1° when used in conjunction with typical f/1.0 optics as discussed in the previous section. The cost factor associated with $\sim 10^3$ discrete detectors of this size (with their associated electronics), which would be required to cover an adequate field of view, becomes a major consideration. There is also a requirement for gain control on the individual pixels which is usually achieved via individual high voltage supplies, though methods have been devised for using a single HV supply feeding all pixel bases, with individual gains adjusted by controlling the current flow in the dynode voltage divider using inexpensive circuitry under computer control (Stamm, Sauerland, and Müller, 1993). For higher resolution, the relatively new technology of multianode PMT's may be a possibility. Other multi-pixel devices are under development, and may find application in this field in the future. Properties of some of these devices are summarised in table III. Several authors have discussed the possibility of using solid state silicon-based devices in place of PMT's to achieve finer granularity in the focal plane. Lorenz (1993) proposes combining a fast image intensifier, an external matrix of avalanche photodiodes (APD's), and high gain amplifiers (to compensate for the relatively low gain of the APD's). An advantage of APD's relative to PMT's is their high quantum efficiency (a factor of three higher than PMT's). At present, however, the intrinsic noise associated with the APD is the main limitation. Basa *et al.* (1992) and Fleury (1993) discuss the possibility of using hybrid photo detectors (HPD's) as replacements for standard PMT's. The photoelectron amplification in HPD's is made within a silicon crystal instead of the usual dynode chain. These devices are still at the developmental stage.

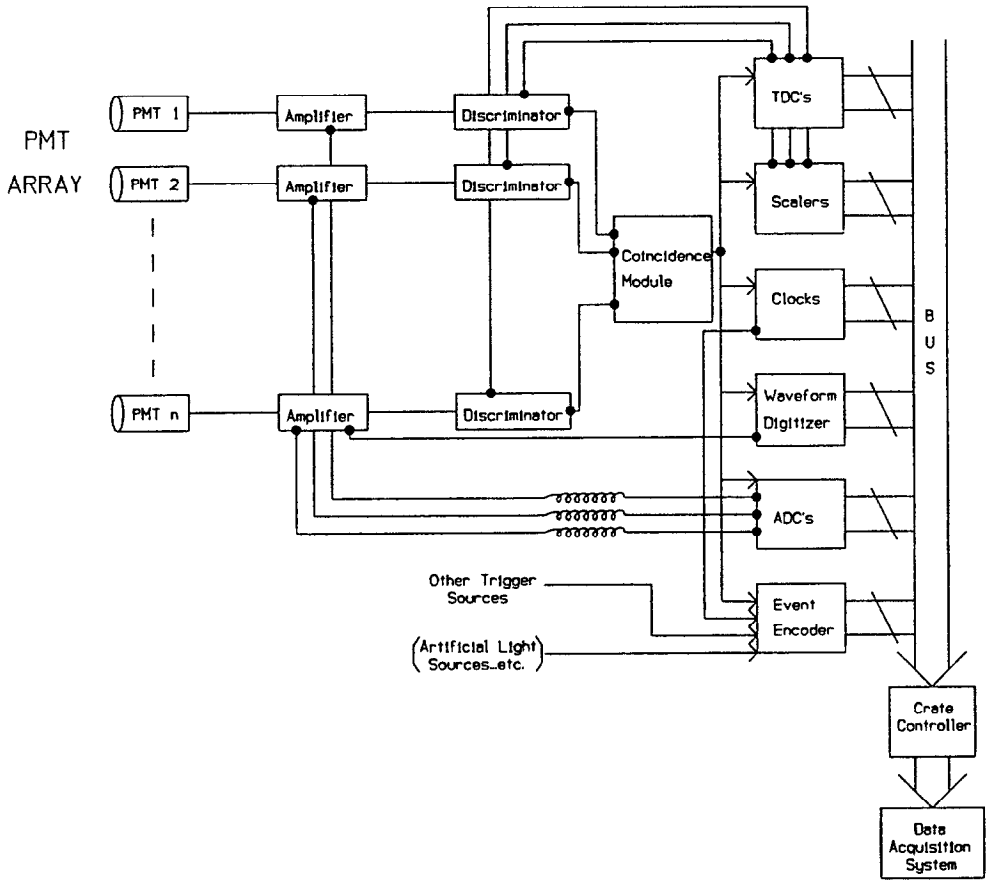

Fig. 2. Block diagram of the data acquisition electronics for a typical atmospheric Cherenkov system.

2.3 Signal Processing Electronics

The high speeds associated with PMT pulses resulting from the registration of an atmospheric Cherenkov light flash dictates the requirements associated with the subsequent processing electronics. In second generation detector systems, it is desirable to preserve the original pulse shape in order to accurately determine the integrated charge (size of the pulse) and possibly the relative timing of pulses from an array of detectors. In some approaches, it is also desirable to quantify the detailed shape profile of the pulse as this may be used to distinguish the nature of the primary particle. A block diagram of the signal processing stages in a typical ACT system is shown in figure 2.

2.3.1 Initial signal amplification

In typical systems, the negative-going pulse from the PMT anode is sent down a 50Ω impedance coaxial cable (e.g. RG58, 1.5dB attenuation per 10m at 100MHz) to a high bandwidth amplifier such as the LeCroy VV100B (×10 gain, 2ns rise-time). The dual output of such a unit permits one signal to be sent to the trigger-forming logic while the other output is sent via a delay to the ADC module where the charge is integrated and digitized. Depending on the mean PMT current due to night-sky illumination, it may be necessary to AC-couple the signal to eliminate DC bias which will vary for different sky regions. For systems where preservation of the risetime or pulse shape are of critical importance, it is usual to amplify the pulses prior to transmission over low-dispersion 50Ω cable such as RG8U (0.5dB attenuation per 10m at 100MHz) (e.g. Resvanis *et al.* 1988).

2.3.2 Trigger formation

The first stage of the trigger-forming logic typically consists of high speed discrimination of the analog pulses. A NIM or CAMAC module may be used to yield NIM or ECL logic pulses of programmable duration if the analog pulse exceeds a preset threshold. Thresholds range typically from −10mV to −1V and output durations may range from 3 to 100ns. Multichannel modules usually provide summed outputs for use in subsequent triggering stages. Individual discriminator outputs or summed outputs are then passed to coincidence logic units or majority logic units where a wide range of trigger criteria may be satisfied; in imaging systems, for example, a trigger of n pixels exceeding threshold out of a total of N pixels may be demanded. As the resulting trigger pulse is used to gate the ADC's and TDC's, care must be taken to ensure that the relative timing of gate and analog pulses does not vary with the trigger multiplicity. Note that the trigger formation relies on voltage amplitudes whereas the information which is recorded in, for example, imaging detectors, is usually the integrated charge under the pulse (section 2.3.3).

In detector systems utilising the fast-timing approach, where accurate time differences between individual analog pulses down to resolutions of 0.1ns are desired, it is customary to use constant-fraction discriminators to generate the timing signals. The input signal is split, and one half is inverted and attenuated while the other half is delayed by a fixed amount. When these two signals are recombined, the zero-crossing point is independent of the input amplitude and may be used as a reference point for timing purposes (Delaney and Finch, 1992).

It is anticipated that future ACT systems will require more sophisticated triggering logic. In large-scale imaging systems, for example, the triggering may be performed on a 'sectored' basis where the imaging array is split into a series of overlapping regions to avoid high rates of accidental coincidences (proposed for the CAT project). 'Intelligent' triggers will also help in this regard: by demanding that the triggering pixels be adjacent, the accidental trigger rates will be reduced, and will permit lowering of the individual threshold settings, resulting in reduced energy threshold. A neural network trigger is also a possible approach, which could

potentially select gamma-ray-like events in hardware.

2.3.3 ADC's for Imaging Systems

Following a delay to allow for triggering formation, the amplified analog pulse in typical imaging systems is sent to a charge analog-to-digital converter such as the LeCroy 2249A 12-channel CAMAC module (e.g. Cawley *et al.* 1990). This ADC uses the Wilkinson charge run-down technique, which initially stores the charge associated with the PMT pulse on a capacitor and then permits the capacitor to discharge at a constant rate. The time taken for the discharge is digitized by gating an oscillator. Ten-bit digitization is typical, with an input sensitivity of 0.25pC/count for a full scale range of 256pC. A common NIM-logic signal which is derived from the trigger pulse is used to gate each ADC channel. Gate durations may range from 10ns to 200ns, with gate sizes of 10 to 30 ns being typically used in ACT systems. A total digitizing time of between 50 and 100μs is normal for such systems, and this is a major contributor to the dead time of the ACT (elsewhere in ACT systems, deadtime limitations are imposed by memory and disk access times). A small residual pedestal (non-zero output in the absence of any analog pulse) is expected from such ADC's, which increases in proportion to the gate duration. It is common in imaging systems to deliberately increase this pedestal value in order that fluctuations associated with the night-sky illumination on the PMT may be quantified (negative fluctuations in the light level will give rise to a distribution of pulses between zero digital counts and the pedestal value). As ACT imaging systems move towards higher resolution, with upwards of 500 pixels in the camera, the CAMAC ADC approach becomes prohibitively expensive and cumbersome. Future systems may adopt the approach of the CANGAROO experiment where customised Cherenkov Circuit Modules have been developed which do all the processing on groups of pixels (ADC, TDC, singles rates monitoring, etc.; Ebisuzaki *et al.* 1991). Alternatively, high-density FASTBUS modules such as the LeCroy 96-channel 15-bit charge ADC may be a possibility. Very high speed flash ADC's are now available from several manufacturers (e.g. Sony, Analog Devices, Datel), and may provide an alternative approach for future imaging systems. These devices, designed for use in applications such as digital oscilloscopes and real-time image processing, typically have 8-bit resolution and bandwidths between 100 and 200MHz. The use of such devices may offer several advantages: the digitized information is the same as what was used to form the trigger (the pulse height, rather than the integrated charge); there would be a considerable reduction in system deadtime; there should be a cost advantage in using flash ADC's over existing approaches.

2.3.4 TDC's for Fast Timing systems

Accurate time-of-arrival information associated with the Cherenkov light front may be utilised in several ways to improve the sensitivity of the ACT. In arrays of detectors, such as with the THEMISTOCLE experiment (Baillon *et al.* 1993a),

the relative arrival time of the light at different detectors is used to reconstruct the arrival direction of the shower front, resulting in an angular resolution of order 0.15°. For this system, a timing resolution of 0.1ns with a full range of 600ns is used. In imaging systems such as CANGAROO which use isochronous mirrors, the timing data from TDC's associated with each pixel may be used to identify Cherenkov photons from background light (Ebisuzaki *et al.* 1991). The resolution in this case is 0.05ns with a full range of 200ns. As discussed previously, accurate start times must be derived from the individual analog pixels which are independent of pulse amplitude, and constant-fraction discriminators are usually used for this purpose.

As a further refinement of fast-timing approaches, some present and proposed systems plan to record the detailed shape of the Cherenkov pulse from a subset of the system channels. Pulse shape data may provide an independent means of discriminating between gamma- and background-initiated events (Tumer *et al.* 1990; Roberts *et al.* 1991). Several approaches are being used to capture the pulse shape. Roberts *et al.* (1991) used a Tektronix 7912 fast transient digitizer to capture the pulse shape with a resolution of 0.5ns and full range of 256ns. Baillon *et al.* (1993a) used a LeCroy 6880A waveform digitizer, with a sampling time of 0.74ns and range of 4μs.

3 System Calibration

Calibration of ACT systems may be discussed in terms of relative calibration (flat fielding of imaging arrays, relative timing between individual elements in an array, etc.) and absolute calibration (energy threshold and collection area). We shall concentrate primarily on the latter, as absolute calibration is essential for inter-system comparison. We shall return briefly to some of the issues involved in relative calibration at the end of this section.

In order to determine absolute source fluxes, it is necessary to calibrate an ACT system both in terms of its threshold energy and its collection area for gamma rays. Due to fluctuations in cascade development, and the fact that collection area varies as a function of energy, neither the energy threshold nor the collection area are easily defined. The collection area increases as a function of energy, but the differential flux (dN/dE) from a source decreases as the energy increases, usually as a power law with some spectral index γ. The product of these two functions will determine the differential rate of events (for an energy between E and $E+dE$) detected from a given source. The effective energy threshold E_E may be defined as the value of E at which $E^{-\gamma}A(E)$ is a maximum (Weekes, 1976), where $A(E)$ is the collection area as a function of energy (alternatively, the median energy can be used to define an effective energy threshold, which results in a somewhat higher threshold value). An effective collection area can be defined as the mean

area associated with showers above E_E:

$$A_E = \frac{\int A(E)N(E)dE}{\int N(E)dE} \tag{9}$$

where $N(E)dE$ is the differential gamma-ray spectrum. Two main approaches are used in determining E_E and A_E for a particular ACT system: Monte Carlo simulations of electromagnetic showers, or a combination of simulations and a direct rate comparison with the observed cosmic ray flux. In the simulations approach, the response of a particular system (optics, focal plane configuration, trigger configuration) is tested against a range of gamma-ray energies (for an assumed spectral index γ) over a range of lateral impact distances. Those events which successfully trigger the system are used to build up the $E^{-\gamma}A(E)$ curve from which E_E and A_E may be estimated (Weekes, 1976). It is still necessary to experimentally determine the absolute gain of the system which relates the photoelectric yield at the photocathode to the digital counts recorded per channel (see below).

The energy spectrum of primary cosmic rays is well determined (e.g. Burnett *et al.* 1990). Thus, if the effective solid angle and collection areas of a particular system are measured or determined from simulations, the threshold energy for cosmic-ray-induced events may be determined by comparing the observed trigger rate with the cosmic-ray spectrum (e.g. Resvanis *et al.* 1988). The energy threshold for gamma-ray events will be less. Much of the primary energy in electromagnetic cascades goes towards producing electron-positron pairs which are efficient generators of Cherenkov light. By contrast, in hadronic showers a significant fraction of the primary energy is converted into muons which will fall below the threshold for Cherenkov light production much sooner than electrons of the same energy. In addition, some of the primary energy goes into the production of other energetic hadrons which are below the Cherenkov threshold, and non-Cherenkov producing mechanisms such as neutrino production and nuclear excitation. The Cherenkov yield of gamma-ray induced showers at 1TeV is about a factor of two larger than for proton-induced showers at similar energies, and this ratio increases at lower energies (Weekes and Turver, 1977). This effect must be taken into consideration when extrapolating the gamma-ray threshold energy from the threshold estimated using the observed cosmic-ray trigger rate.

A variety of methods are used to determine the absolute gain of an ACT system, which is an essential step in determining the threshold energy and spectral response of the system. Most of these approaches measure the overall gain of the system by injecting a known amount of light into individual PMT channels and measuring the resulting digital response at the final stages of the data acquisition system, resulting in a photoelectron to digital count conversion factor. Scintillators coupled to calibrated alpha-particle sources may be used as sources of fast light pulses of known size; used in conjunction with the known quantum efficiency response of a particular PMT, these give a predetermined number of photoelectrons which can be sent through a channel to determine its response in digital units.

Gorham (1986) describes an alternative approach using a muon telescope/acrylic light pipe combination to produce Cherenkov pulses of known size. The telescope triggers only for cosmic ray muons which give rise to Cherenkov photons which propagate along the long axis of the pipe, which is coupled to the PMT face. This configuration yields a calculable number of photons per pulse. For systems capable of operating at the single photoelectron level (narrow field of view per pixel, coupled to relatively small mirror areas) the background night sky may be used to calibrate the discriminator threshold settings and subsequent digital unit conversion. The single channel counting rate due to the night-sky light is monitored as a function of discrimination level; a plateau in the counting rate indicates the detection of single photoelectrons (Kifune *et al.* 1993).

All of these methods yield an estimate of the photoelectron to digital count conversion factor, but the uncertainties associated with atmospheric absorption of the Cherenkov light, and the response of the telescope primary optics, must still be folded into the simulations. Ideally, one would like to have an atmospheric Cherenkov light source of known intensity to illuminate the telescope and thus measure its response in terms of digital counts as if during normal operation. Vacanti *et al.* (1994) propose using the Cherenkov ring images associated with high energy muons travelling in the vicinity of the telescope for this purpose. This method is specifically designed for Cherenkov imaging systems, which may recognise the local muons via their ring signature. The light distribution varies only as a function of the muon's distance of impact from the telescope and the muon energy. If this distance is known, by, for example, triggering the system using an independent muon telescope placed beside the Cherenkov imaging telescope, then one can predict the signal seen by each pixel of the camera and compare it to the actual response to obtain the conversion factor. This method of calibration, suggested by Hillas and Patterson (1990), has been used by the Whipple collaboration (Jiang *et al.* 1993) and the Adelaide group (Rowell *et al.* 1991) to calibrate their telescopes.

The energy resolution of an ACT determines how accurately one can estimate a source energy spectrum, which is the critical observation providing insight into the physics of the source acceleration mechanism and into the properties of the interstellar and intergalactic media (via absorption and cutoff features in the spectrum). The telescope energy resolution function is typically determined from Monte Carlo simulations (Lewis *et al.* 1991; Chilingarian *et al.* 1991). To date, efforts at determining source spectra from Cherenkov data have mainly concentrated on the Cherenkov imaging technique. There is a strong linear correlation between the number of Cherenkov photons recorded in an image and the gamma-ray primary energy (assuming that none of the image is missed). There is also a weaker energy dependence on the distance of the image centroid from the source location. Using these dependencies as determined from a large family of simulated Cherenkov images, an energy can be assigned to individual observed events with an estimated uncertainly of order 25 – 30%. In general, the collection area will change as a

function of energy, and this must be taken into consideration when determining source spectra. The collection area will also change as a function of detector trigger mode and may also depend on the selection criteria used to isolate gamma-ray candidate events. For spectral analysis, it is preferable to use selection criteria which are independent of energy, even though such cuts may not yield the most enriched gamma-ray sample (Lewis *et al.* 1991).

Apart from determining the effective threshold energy and collection area of a particular system, it is also essential to calibrate system channels relative to each other. In imaging systems, this consists of 'flat-fielding' the pixel array, i.e. determining relative gain factors to equalise the response across the entire field of view. Several approaches are used in practice. The Whipple group employ a fast nitrogen flash lamp to uniformly illuminate the focal plane array with fast (5ns) pulses of blue light whose spectral characteristics closely match the atmospheric Cherenkov light spectrum. A file of these artificial triggers is recorded at the start of each night, and used to determine relative gain factors for all pixels for the night in question (Cawley *et al.* 1990). The gain factors have been compared with independent factors derived from the averaged responses of pixels to many atmospheric Cherenkov images, on the assumption that all pixels at the same radius relative to the centre of the field of view should detect the same aggregate Cherenkov light over several hours of observations. Good agreement is found between these two approaches. Other groups employ fast laser pulses (Mirzoyan, 1992; Baillon *et al.* 1993b) or pulsed LED's (Hara *et al.* 1993) to determine relative gain factors. Laser pulses are also used to accurately determine relative delays between channels in fast timing arrays (Baillon *et al.* 1993b).

4 Different Methodologies

The key to progress in VHE gamma-ray astronomy lies in (a) detecting the gamma-ray air shower with high efficiency and (b) distinguishing gamma-ray showers from a discrete source from showers generated by the isotropic background of hadrons in the cosmic radiation. Other backgrounds are the cosmic electron background and the diffuse gamma-ray background; at present there is no way to distinguish an electron-initiated electromagnetic cascade from a photon-initiated one. With current systems these are not limiting factors since their fluxes are $< 10^{-3}$ and 10^{-4} of the hadronic flux at the same energies but projected systems may well be effectively limited by the diffuse electron background.

The largest gamma-ray telescope flown to date (the EGRET experiment on the Compton GRO) has a collection area at its highest energy (30 GeV) of less than $10^3 cm^2$; the simplest atmospheric Cherenkov detector (with energy threshold of 1 TeV) has a collection area of $5 \times 10^8 cm^2$. This collection area is determined by the inherent diameter of the Cherenkov light pool at detector level and is not determined by the size of the light detector. The power of the ground-based technique lies in this differential in collection area between space and atmospheric

Cherenkov detectors; this is the factor that compensates for the fact that the primary photon does not get any closer to the detector than 20 km and that the air shower must be detected in the presence of background light from the night-sky, from man-made sources and, in particular, from Cherenkov light from cosmic-ray initiated air showers. It is important that whatever method of Cherenkov light detection is employed it does not reduce this large collection area by a significant amount.

Discrimination against the hadronic background comes in one of three ways — intensity, angular resolution, and shower parameter differentiation. In a particular installation, several of these discrimination approaches are usually used in combination.

4.1 INTENSITY

It is well known that air showers produced by hadrons are less efficient in the production of Cherenkov light than their electromagnetic counterparts with identical energy in the primary. The most efficient producers of Cherenkov light are electrons which are just above the Cherenkov threshold; hence a shower which develops with the highest possible fraction of the total energy in this electron component is the most visible to Cherenkov light detectors. Over most of the 0.1 to 10 TeV energy range the ratio, κ, of Cherenkov light output from a gamma-ray shower to that from a proton shower is a factor of 2–3 (the exact factor depends on the detector parameters, elevation, etc). From section 1, equation (7), the flux sensitivity (in standard deviations) may be expressed as

$$N_{sig} \propto \frac{E_g^{-G}}{\sqrt{E_b^{-1.7}}} \tag{10}$$

where E_g and E_b are the threshold energies for gamma-rays and protons, respectively. As discussed above, these thresholds will be different due to different Cherenkov light yield efficiencies. If $E_g \propto C_T$ where C_T is the threshold Cherenkov light yield for triggering a particular detector (in photons per square meter), then $E_b \propto \kappa C_T$, and thus

$$N_{sig} \propto C_T^{0.85-G} \kappa^{0.85} . \tag{11}$$

At energies below 100 GeV the ratio κ increases dramatically (figure 3). This may be explained as follows. In a proton shower most of the Cherenkov light comes from the secondary electromagnetic cascades. Energy comes into these cascades via the production of pions by the primary and the subsequent nucleon cascade. Two thirds of the energy (approximately) goes to charged pions; they can decay to muons or undergo collision. The latter process is a more efficient method of producing Cherenkov light; since the lifetime against decay is greater at higher energies, the chance of collisions is greater. At lower energies therefore, proportionally more energy comes off in muons whose energy may be below the

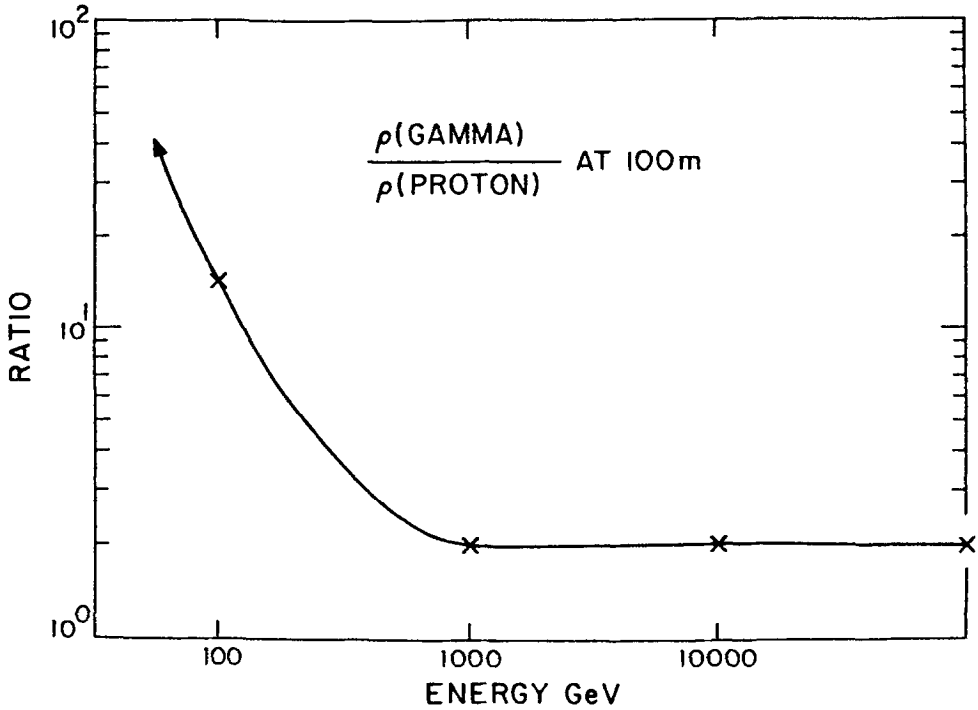

Fig. 3. The density of Cherenkov light at detector level from a vertically incident gamma-ray and proton shower at a radial distance of 100m from the shower axis is plotted as a function of primary energy (Weekes and Turver, 1977).

Cherenkov threshold and hence the low energy showers are deficient in Cherenkov light (Weekes and Turver, 1977).

Although this would seem to justify a strong push to lower energies it should be remembered that as Cherenkov detectors become more sensitive they become better detectors of single muons which may replace hadronic showers as the major source of background.

4.2 Angular Resolution

If the background is isotropic and the source is point-like, there is a clear advantage in increasing the angular resolution of the atmospheric Cherenkov telescope. Fortunately the electromagnetic cascade is a tighter entity which is far more easily characterized than its hadronic counterpart; its axis is an accurate projection of the trajectory of the primary gamma-ray and the shower wavefront is symmetric about this axis. The angular dimensions of the Cherenkov light spot and the dis-

placement of the shower centroid from the gamma-ray trajectory as seen from the detector is about 1° so that Cherenkov detectors have an inherent resolution of 1–2°.

Two methods of improving the angular resolution are generally considered: image projection and wavefront timing. In the former the angular distribution of the light is measured, preferably with more than one detector. In the latter the time of arrival of the wavefront is sampled by many small detectors, whose separation is comparable to the shower dimensions.

4.2.1 Image Projection

The Cherenkov light image of a gamma-ray shower (centered in the field of view) can be recorded by an imaging device (usually a collection of photomultipliers, although image intensifiers, read by CCD's, have also been discussed as possible detectors (Mattox, 1988)). The orientation of the roughly elliptical image of the shower depends on the angle it makes with the optic axis of the telescope; showers which are parallel to the axis but fall up to 120m away have elliptical images whose major axis intersect the optic axis (figure 4). This is the same geometrical principle that causes the trails of meteors to point back to their common radiant. This holds true for gamma-ray and hadron showers but it is easier to characterize the axis of a gamma-ray shower because of the tighter image.

By determining the major axis of the elliptical image the position of the source can be determined in one dimension. The ellipticity of the image is a function of the impact parameter so that position can be limited to a displacement from the centroid along the axis. By consideration of the third moment the ambiguity in the direction of the displacement can be removed (Lang, 1991).

The angular resolution of such an imaging device depends primarily on the pixel size and inter-pixel spacing, assuming that the pixels are not smaller than the smallest structures within the Cherenkov image (below this limit, decreasing the pixel size will not improve the resolution as no new information is recorded). It is found that the angular resolution for an individual Cherenkov flash is approximately half the pixel size (i.e. this is the accuracy to which the pointing of the major axis of the image may be determined). Thus, for a point source, the angular resolution of the Whipple Collaboration 10m instrument is $\sim$0.13°, which corresponds to the mean 'miss' value of events accepted in the gamma-ray domain ('miss' is the angular perpendicular distance of the major axis of the image from the source location). For the CANGAROO imaging camera, the pixel size is 0.14° and the angular resolution is quoted at 0.1° (Kifune *et al.* 1995). Hillas (1989) has shown using simulations that individual event resolution of a few arcminutes should be attainable given sufficient pixel resolution. Averaging over many gamma-ray candidate images reduces the source location error to a point where systematic errors, such as tracking and encoding errors, dominate. Sources have been located to an accuracy of 5' (0.08°) using this approach (Akerlof *et al.* 1991).

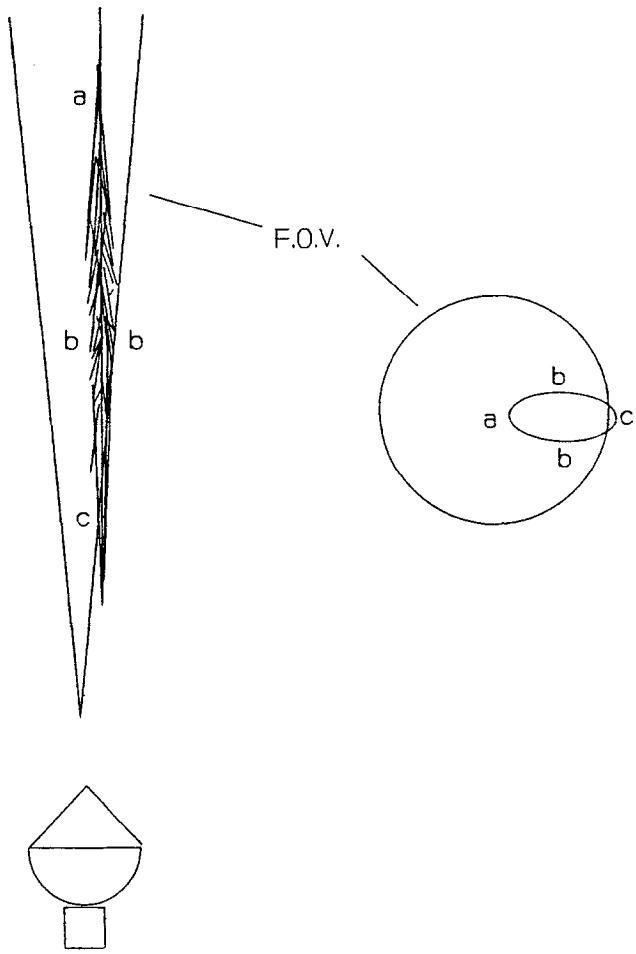

Fig. 4. Schematic depiction of the development of an air shower and the roughly elliptical image that it produces in an imaging Cherenkov detector.

4.2.2 Wavefront Timing

Air showers can be detected by an array of small optical telescopes separated by distances from 10 to 100m and operated in coincidence. The individual elements can be bare phototubes, tubes with light cones and baffles or mirrors with phototubes at their foci. The shower arrival direction is determined by the relative time of arrival of the optical shower front at the individual detectors. In this respect the technique is very similar to that used in particle air shower arrays; the angular resolution is determined by the thickness of the shower front and the speed of the electronics.

The detecting elements are invariably a compromise; if there are many, then economics dictate that they be small and hence the energy threshold is increased. If they have wide fields of view, then the area of sky surveyed is large but again their thresholds are increased. This approach was originally used at Bowie State College (Tornabene and Cusimano, 1968) but has been used recently by a number of groups: Durham (Dowthwaite *et al.* 1984), Sandia (Akerlof *et al.* 1989), ASGAT (Goret *et al.* 1993), THEMISTOCLE (Baillon *et al.* 1991) and AIROBICC (Karle *et al.* 1991). The angular resolution associated with this technique declines with decreasing shower energy, as the Cherenkov light wavefront changes from conical to spherical shape (M. Urban, private communication).

4.3 Shower Parameter Differentiation

The development of a hadron and gamma-ray shower is quite different as can be seen from figure 5 which shows a Monte Carlo simulation of two typical air showers. It is apparent that the hadron shower is more penetrating and has a greater spread (due to the inherently larger opening angle of hadronic interactions compared with electromagnetic interactions). The measurable properties of the two types of air shower are also different as can be seen from figure 6 which illustrates the typical profiles of the two types of shower as regards their lateral distribution on the ground around the shower axis, their time profiles, the spectral distribution of the light, and the angular distribution of the light as seen projected on the sky. Each of these properties has been used to exploit the differences in the signal beam of gamma rays and the isotropic background of charged cosmic rays.

4.3.1 Lateral Distribution

The gamma-ray shower is expected to have a flatter distribution than the equivalent proton shower; hence some discrimination can be achieved if the densities are recorded over an array of detectors whose separations are such that the shower light pool is effectively sampled. The degree of discrimination that can be achieved in this way has not yet been fully calculated. All Cherenkov telescopes which employ two or more separated detectors benefit from this discrimination to some degree; it is the principal discriminant to be used in the detector now under construction by the Tata Institute at Pachimari (Vishwanath *et al.* 1993).

Some successes have been recorded with these approaches but these have come mainly from an improvement in the angular resolution of the technique, and no experiment has achieved a background rejection that is more than 99% efficient. At lower energies (10–100GeV) the lateral distribution of the light from a gamma-ray shower is dominated by the ring at radius 100–120m; this feature may be the most important discriminant at these energies (e.g. Krys *et al.* 1991).

4.3.2 Duration

The light-pulse from a gamma-ray shower is shorter than that from a hadronic shower. The use of time duration to discriminate the faster light pulses of gamma-

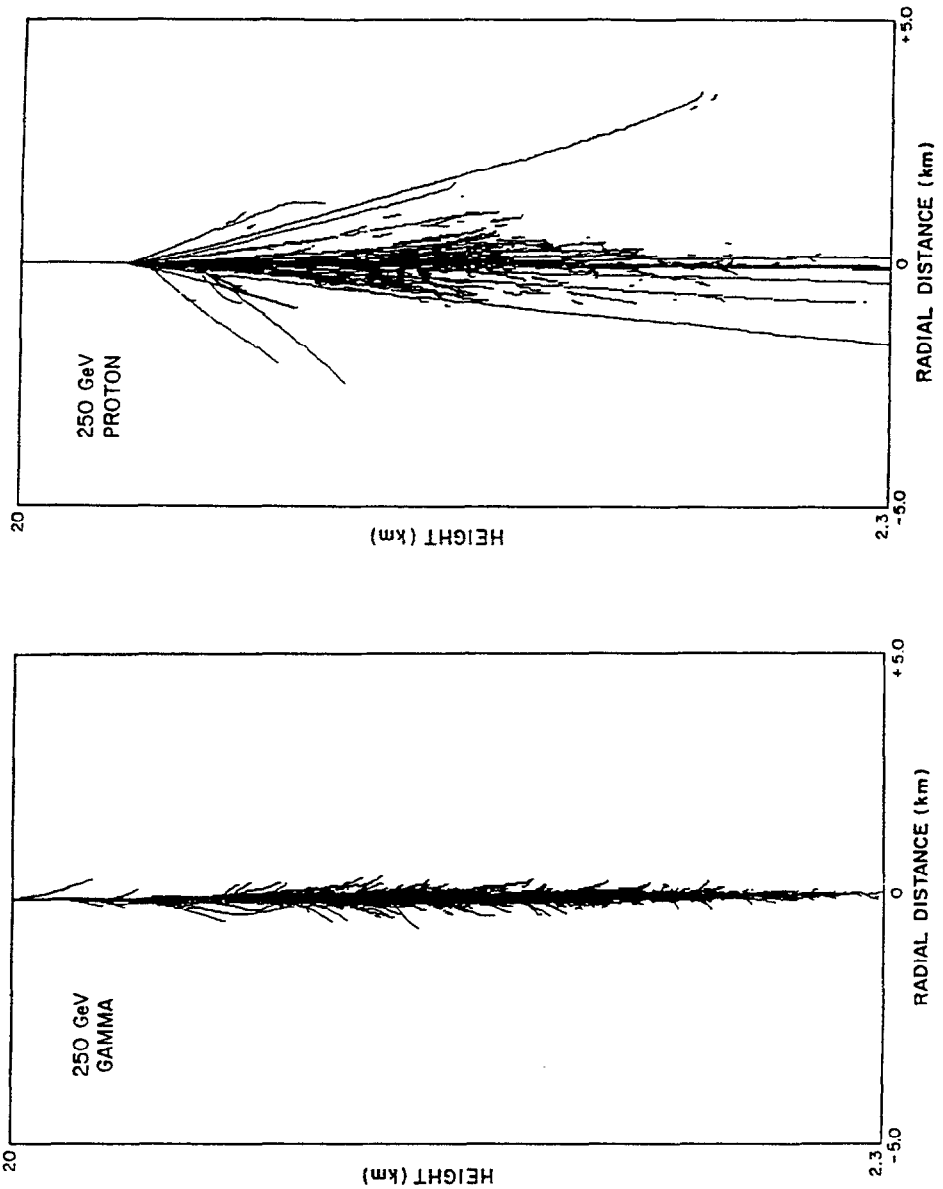

Fig. 5. Monte Carlo simulation of the development of showers initiated by a gamma ray and proton primary of 250GeV; each track represents a particle radiating Cherenkov light (G. Sembroski, private communication).

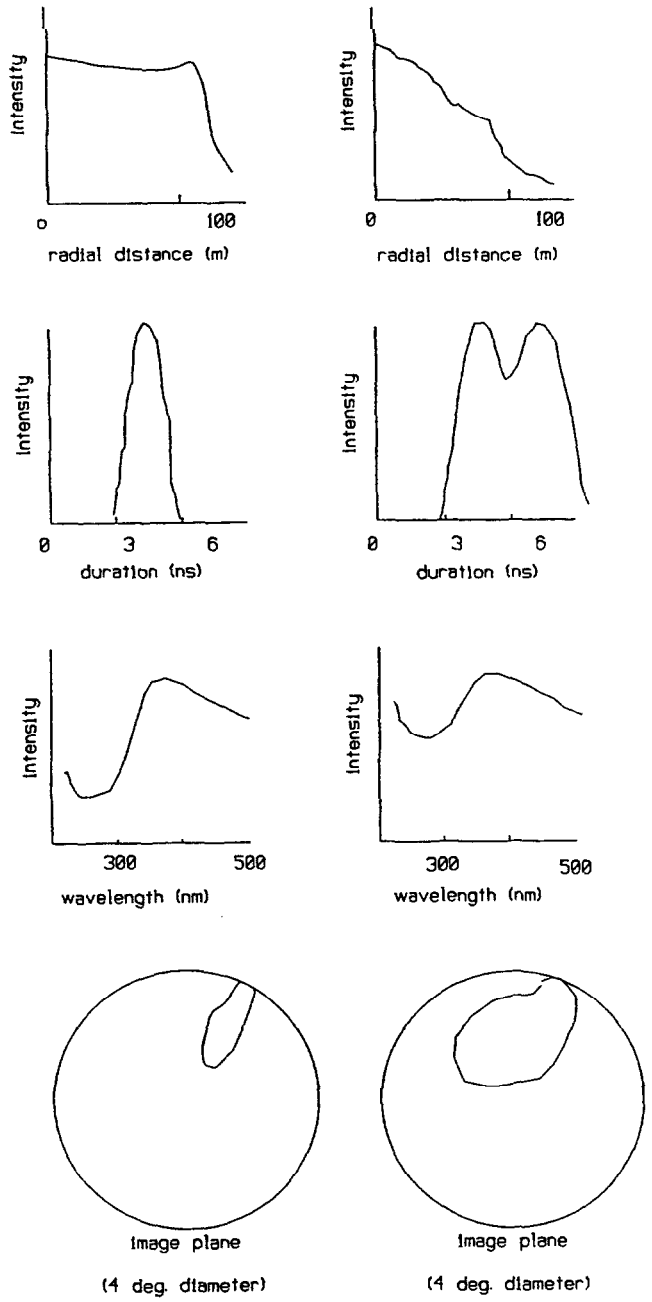

Fig. 6. Schematic depiction of the differences in a typical shower initiated by a gamma ray and a proton.

ray showers from those slower pulses of the background hadronic showers had its most serious application in the Haleakala experiment (Resvanis *et al.* 1986) where it was to be the prime discriminant; the system consisted of 26 individual parallel telescopes. However it is difficult to use this discriminant alone to detect a gamma-ray signal from a source. The Haleakala experiment has recently been reassessed (Morse *et al.* 1993); the efficiency of the technique was found to be limited by the optical quality and alignment of the individual telescopes. The same technique is used in the South Pole GASP experiment with 10 parallel telescopes (Tilav *et al.* 1993). All Cherenkov detectors utilize this timing discriminant to some degree by matching the time constant of their detectors to the thickness of the wavefront (1–3 ns).

4.3.3 Color

Since there are more local (penetrating) particles in the hadronic shower the Cherenkov light is less attenuated than that in an electromagnetic cascade. The attenuation is strongest in the blue and ultraviolet so that it should be possible to discriminate against hadronic showers on the basis of the ultraviolet-to-visible ratio, i.e. the local particles in the hadronic showers contribute a greater proportion of ultraviolet light. This approach was used as a discriminant in the Smithsonian "Double Beam" experiments (Grindlay, 1972) and is a major part of the Crimean imaging system in which there are three visible cameras and three ultraviolet detectors (Vladimirskii *et al.* 1989). Recently the Crimean group reported the detection of a signal from the Crab Nebula using this discriminant in combination with the size of the shower images (Kalekin *et al.* 1994). All Cherenkov experiments try to match the spectral response of their triggering detectors to the spectral distribution of the light from a gamma-ray shower (Goret *et al.* 1993); however in imaging detectors the angular distribution of the ultraviolet component is an indication of the hadronic nature of the primary. Ideally the trigger should be sensitive to the visible but the image recorded by the camera should be equally sensitive to the visible (for axis determination) and ultraviolet (for identification of the primary).

Two experiments have been designed to operate solely in the ultraviolet: the ARTEMIS experiment (Urban *et al.* 1990) which uses solar-blind photomultipliers in the Whipple imaging camera and the CLUE experiment (Anassontzis *et al.* 1992) which uses TMAE chambers in an array of 1.8m optical reflectors. These experiments aim to operate at wavelengths below 300nm so that they are insensitive to moonlight and hence can potentially extend the useful duty cycle of ground-based optical detectors by a factor of two. However it is difficult to characterize the shower arrival directions from local particles and there is an inherent bias towards the detection of hadronic showers and muons.

4.3.4 Imaging

The most successful discrimination technique appears to be the imaging method by which hadronic showers are identified and rejected with 99.7% efficiency, while

retaining about 60% of the gamma-ray signal. Originally this imaging method was considered primarily as a means of increasing the angular resolution (Weekes and Turver, 1977); it was only later that the possibility of using the images to identify the primary was realized (Weekes, 1981; Hillas, 1985).

Although the image could be recorded on any of the imaging devices currently used in two-dimensional astronomical photometry, an array of small phototubes is the best match to the crude optics of the collectors, the short duration of the light flash, the high data rate, and low contrast images expected from air showers. The first imaging camera was developed by the Whipple Observatory Gamma Ray Collaboration and consisted of 37 pixels (5 cm diameter phototubes) spaced 0.5° apart with a full-field of 3.5°; a similar camera was developed at the Crimean Astrophysical Observatory (Vladimirskii *et al.* 1989). The current imaging systems used by the Whipple Observatory Gamma Ray Collaboration are discussed in section 5.1. There are also noteworthy developments in imaging systems 1) in Woomera, Australia by a joint Australian-Japanese collaboration, the CANGAROO experiment (Ebisuzaki *et al.* 1991) and 2) in the Canary Islands by an Armenian-German collaboration, the HEGRA experiment (Aharonian *et al.* 1991a). There are also proposed imaging experiments in Narrabri, Australia (University of Durham, United Kingdom) (Bowden *et al.* 1993), in Tien Shen, Alma-Ata, by the Lebedev Institute, Russia (Sinitsyna *et al.* 1993) and at Themis, France by a French collaboration (Degrange *et al.* 1993).

5 Existing Gamma-ray Telescopes

There are currently more than twelve VHE atmospheric Cherenkov gamma-ray telescopes in operation (or about to come into operation) (table IV); most of these are second-generation instruments which are defined as those which provide effective discrimination against the cosmic ray background. One first generation telescope is particularly noteworthy; the South African experiment at Nooitgedacht relies on the use of multiple, relatively small, telescopes, operated independently, to increase the gamma-ray collection area and hence the sensitivity to weak fluxes (Raubenheimer *et al.* 1993).

In general all of the telescopes in table IV have collection areas determined by the size of the Cherenkov light pool, 3×10^8 to $5 \times 10^8 cm^2$. Ideally they are located on mountain tops with desert climates. As with all ground-based instruments only one hemisphere of the sky is visible to an individual telescope.

Four atmospheric Cherenkov telescopes are briefly considered in more detail, followed by a review of some of the systems operating at higher energies (> 50TeV).

5.1 Whipple Telescopes

The first imaging camera was developed by the Whipple Observatory Gamma Ray Collaboration and was designed around the Whipple Observatory 10m optical reflector; in its present form (Cawley *et al.* 1990) it uses a camera head consisting

TABLE IV
Some Atmospheric Cherenkov Observatories c.1994.

Experiment or Organization/ Location	Long.	Lat.	Elev. (km)	Thres. (TeV)	Technique
SPASE, South Pole		90S	2.5	0.5	Duration
Potchefstroom, South Africa	27E	27S	1.4	1.0	Conventional
CANGAROO, Australia	137E	31S	0.0	1.0	Imaging
Durham, Narrabri, Australia	150E	30S	0.2	0.1	Imaging
CAO, Crimea, Ukraine	34E	45N	0.6	1.0	Imaging
Lebedev, Tien Shan, C.I.S.	75E	42N	3.3	1.0	Imaging
HEGRA, La Palma, Spain	18W	29N	2.2	0.5	Imaging
Whipple Collab., U.S.A.	111W	32N	2.3	0.2	Imaging
IHEP, Beijing, China	117E	40N	1.0	1.0	Conventional
THEMISTOCLE, France	1W	43N	1.5	3.0	Timing
CAT, France	1W	43N	1.5	0.2	Imaging
CLUE (Pisa), La Palma, Spain	18W	29N	2.2	0.5	UV
Tata, Pachmari, India	78E	22N	1.1		Lateral
TACTIC, Mt. Abu, India	73E	24N	1.7	0.2	Imaging

of 109 phototubes with typical spacing 0.25° (figure 7). Upon command the light level at each pixel is digitized and recorded. The Cherenkov light image of each air shower is recorded at a trigger rate of 5 Hz. Some typical images are shown in figure 8. The effective energy threshold is about 0.3 TeV and the gamma-ray collection area is about $3 \times 10^8 cm^2$.

The initial method used was based on the use of a single parameter which combined the two distinguishing aspects of the gamma-ray events i.e. the so-called Azwidth parameter (Hillas 1985; Weekes *et al.* 1989). The currently favored approach ("Supercuts" (Punch *et al.* 1991)) has been applied to the analysis of observations of a large number of candidate sources. With this method it has been found possible to retain at least 50% of the gamma rays with rejection of more than 99.7% of the background (Reynolds *et al.* 1993). Part of this selection comes in hardware selection since the triggering criterion, that two of the 0.25° diameter phototubes exceed a preset threshold, preferentially triggers on the showers that have smaller angular extent.

A number of alternative methods have been developed for separating out the gamma-ray events; initially these were based solely on Monte Carlo simulations but later as sources were established it was possible to use the data-bases, such as that on the Crab Nebula (Vacanti *et al.* 1991), to optimize the selection procedures. The analysis methods include: Neural Networks (Reynolds, 1991; Halzen *et al.* 1991); Multivariate (Chilingarian and Cawley, 1991; Hillas and West, 1991; Aharonian *et al.* 1991b; Danaher *et al.* 1993).

The Whipple 10 m camera has been augmented by an 11 m optical reflector which is equipped with a similar camera (Schubnell *et al.* 1992); the second tele-

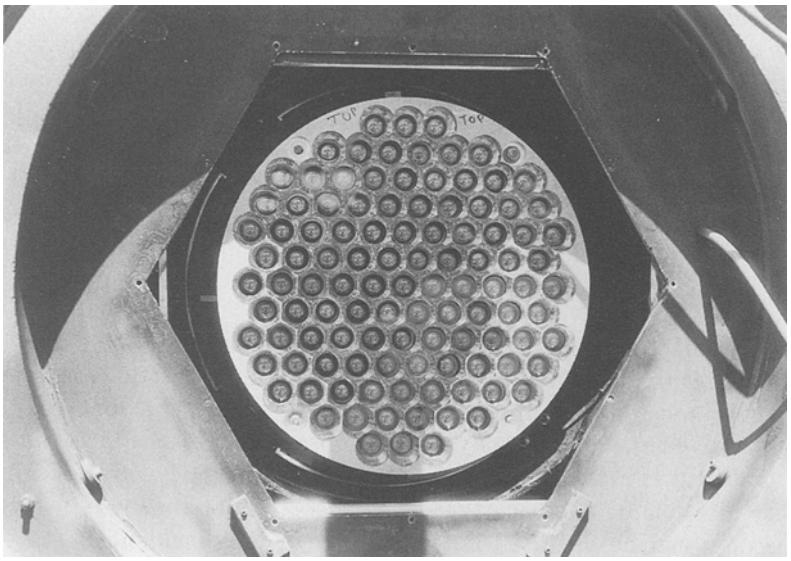

Fig. 7. The camera head of the 10m optical reflector of the Whipple Observatory showing the 109 pixels.

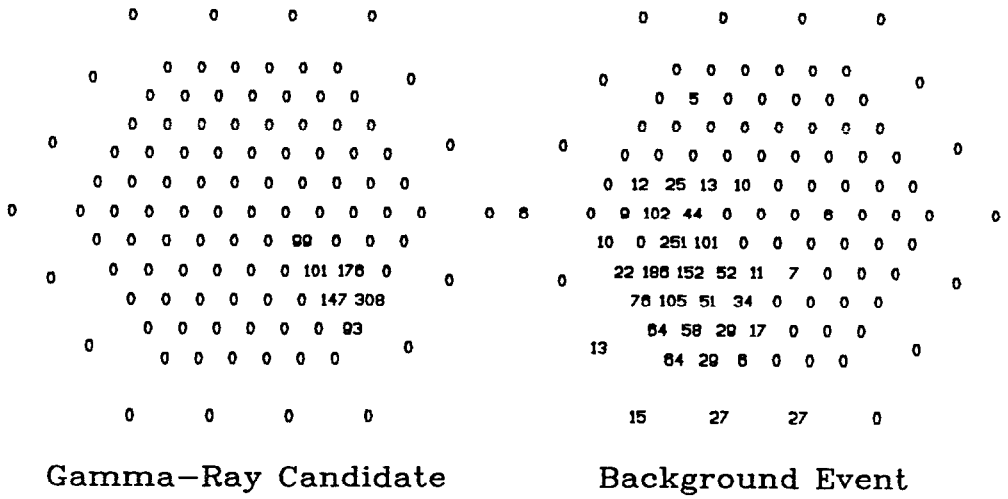

Fig. 8. Typical images recorded by the Whipple 109-pixel camera; the numbers refer to detected photoelectrons.

scope is located 140 m from the 10 m reflector and the two telescopes will operate in coincidence to record stereoscopic images of air showers. The combined system will have an effective energy threshold of 0.1 TeV and a flux sensitivity that is at least a factor of a hundred below that of that of a conventional non-imaging telescope. Hence it should be possible to detect sources whose emission strengths are 1% of that of the Crab Nebula. The Whipple group plan to upgrade the camera on the 10m reflector to 541 pixels, giving both better angular resolution (due to smaller pixels) and a wider field of view to facilitate searches for diffuse sources and to survey large regions of the sky.

5.2 CANGAROO

This stereoscopic telescope is currently the most sensitive VHE system in the Southern Hemisphere; CANGAROO is an acronym for the Collaboration of Australia and Nippon for a Gamma-Ray Observatory in the Outback and, as such, is more descriptive than most acronyms. The observatory site is at Woomera in central Australia. It is made up of two independent telescopes, one developed by the University of Adelaide and the other by a consortium of Japanese institutions; the two telescopes can be operated independently or in coincidence. The Australian telescope, BIGRAT, has been in operation since November, 1988; it consists of three reflectors each of diameter 4m. This hybrid telescope has recently had a 37 pixel camera mounted on its central reflector.

The most exciting results have come from the advanced imaging camera on the Japanese telescope (figure 9); this telescope has been in operation since February, 1992 (Hara *et al.* 1993). The basic optical element is a high quality 3.8m diameter mirror (previously used in lunar laser ranging) which is mounted on an accurate alt-azimuth mount. The camera has 220 pixels (but may be expanded) with a full field of 3°; each square pixel is 0.14° (8 mm). The custom-made circuit modules each consist of 16 channels of amplifiers, discriminators, scalers, ADC's, TDC's, current monitors and adders. A trigger is generated when an individual channel and the sum of adjacent channels exceed preset thresholds which are determined empirically to favor the detection of gamma-ray showers.

The high resolution of the camera and optics permits the imaging technique to be fully exploited; the sensitivity is limited primarily by the poor reflectivity of the mirror, the slow time resolution and the limited aperture. The trigger rate is about 1 Hz and the energy threshold is 1 TeV. This group has recently been funded to build a new high quality imaging telescope with 10m aperture.

5.3 DURHAM

The University of Durham has deployed a new telescope at Narrabri in south-eastern Australia (Bowden *et al.* 1993). It consists of three parabolic composite mirrors (f/1.0), each of 7m aperture, on a single alt-azimuth mount. Using this large collection area in conjunction with Winston cones and albedo light shields, it is hoped to achieve an energy threshold of 60GeV (significantly lower than any

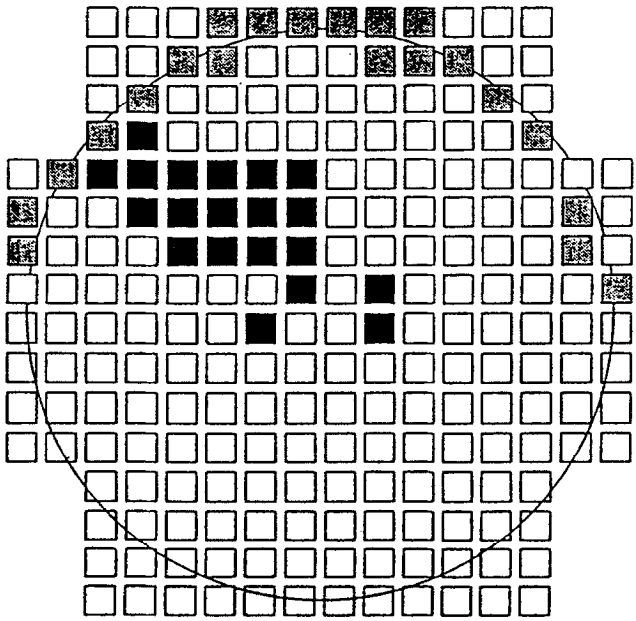

Fig. 9. A typical event seen by the 220-pixel camera of the CANGAROO telescope. The triggered pixels are shown as black squares and the path of a star is shown by the grey squares.

previous atmospheric Cherenkov telescope). The central mirror has a 109-pixel camera in its focal plane (0.25° pixel pitch; 3° full field of view) and each outer mirror has 19 0.5° aperture clustered PMT's. Two trigger modes will be used — a 3-fold fast coincidence between corresponding pixels in each of the 3 cameras, and a trigger involving two or more pixels in the high resolution central camera.

5.4 CAT

Various French institutions which have been involved in the development of the atmospheric Cherenkov technique e.g. ASGAT, THEMISTOCLE, have joined forces to develop a new imaging telescope with high resolution. The 5m aperture telescope will be located at Themis in southern France. It will have a camera with more than 500 pixels, each a photomultiplier of 1 cm diameter (0.1°). The anticipated energy threshold is 200 GeV. It should be operational in 1996.

5.5 Air Shower Arrays

At higher energies (> 50 TeV) there have been significant advances in gamma-ray detector sensitivity. There are now more than a dozen major air shower gamma-ray arrays in operation world-wide including the Cygnus experiment at Los Alamos, the CASA-MIA array at Utah and the SPASE experiment at the South Pole.

The results at these high energies have been somewhat disappointing; despite the increased sensitivity of these experiments the early reports of the detection of 100 TeV signals from the X-ray binaries (Cygnus X-3, Hercules X-1, etc.) have not been confirmed. Emphasis in the operation of these arrays is now shifting to investigation of the composition in the 0.1 to 10 PeV energy region.

Particular mention must be made of the joint Chinese-Japanese high altitude air shower array in Tibet which has an energy threshold of 10 TeV, thus overlapping with the atmospheric Cherenkov experiments.

A completely different experimental approach is provided by the MILAGRO experiment now under construction at Fenton Hill, near Los Alamos, New Mexico (Sinnis, 1992). The water Cherenkov technology developed for the IMB experiment is combined with a conventional particle array to give a gamma-ray experiment; the telescope is built around a large (existing) water reservoir with elements of the disassembled Cygnus array surrounding it. Because the water detector samples a large fraction of the surviving particles in the shower the energy threshold for gamma-rays is low (about 1 TeV) compared with conventional air shower arrays. Discrimination against hadron showers is provided by the deep water detectors which respond primarily to penetrating muons.

The principal advantage of this kind of detector is that it operates full-time with a large opening angle; hence it is well suited for the study of transient sources in the 1–10 TeV energy range. It has also strong sensitivity to gamma-ray bursts. One disadvantage of the MILAGRO experiment is that it operates above what now appears to be the optimum energy range (due to the energy cutoff for distant sources as a result of gamma-ray absorption by photon-photon interactions with the cosmic IR background). On the other hand its range of sensitivity closely matches that of the neutrino telescopes and previous experience shows that each band of the electromagnetic spectrum has its own surprises.

6 Future Directions

The last decade has seen VHE gamma-ray astronomy become a truly observational astronomical discipline which effectively complements the sensitivity demonstrated by the telescopes on the Compton GRO. Although the roster of sources detected at TeV energies is still small it is diverse and has great promise for the future. There has been a significant improvement in ground-based telescope sensitivity but the number of telescopes with this sensitivity is still small and only a small fraction of the sky has been surveyed with high sensitivity.

In most branches of astronomy the growth has been dramatic once the threshold for detection of real and verifiable sources has been achieved; with the detection of the Crab Nebula the threshold has been achieved. Using the Crab Nebula as a standard candle (visible to telescopes in both the northern and southern hemispheres) it has been possible to optimize detection techniques and to cross-calibrate different observing strategies.

However this is not a one source discipline; the VHE source catalog now includes PSR1706-44 (a pulsar/nebula detected by EGRET) (Ogio *et al.* 1993), Markarian 421 (the closest AGN detected by EGRET), (Punch *et al.* 1992), the binary X-ray source, Vela X-1 (North *et al.* 1987; Carramiñana *et al.* 1989), and the cataclysmic variable, AE Aquarii (de Jager *et al.* 1990; Bowden *et al.* 1992). There is considerable diversity in these sources: whereas the Crab Nebula and PSR1706-44 are apparently steady sources at TeV energies, the other three are definitely variable with periodic episodic emission from Vela X-1 and AE Aquarii and flares on a time-scale of a few days seen from Markarian 421. These sources may be the brightest members of their different source categories so that improvements in observing sensitivity guarantees an increase in the number of sources detected.

Particular mention must be made of the only extragalactic source detected, Markarian 421. Although it is one of the weakest AGN's detected by EGRET (in both apparent and absolute luminosity), it is the only AGN that is seen at VHE energies. Because it is also the closest EGRET-detected AGN the suspicion is that the fact that it is observable is due to a lack of absorption (by pair production on the intergalactic infra-red background); it is possible to use the observation to set a limit on the infra-red background and it has even been suggested that observations of other, more distant, AGN's would provide a measure of the Hubble Constant and the era of galaxy formation (Salamon *et al.* 1994; MacMinn and Primack, 1995).

It is imperative, therefore, that telescopes that operate in the 100–1000 GeV energy range be extended so as to build on the successes achieved to date. The angular resolution, energy resolution and field of view of imaging telescopes can be improved by the use of more sophisticated electronic cameras. Such cameras will entail modest improvements in reflector optics, camera electronics and expansion of the number and resolution of pixels; no major technical advances are required.

With a relatively major investment (by the standards of non-accelerator physics) the atmospheric Cherenkov technique can be extended to energies as low as 10 GeV where the sources detected by the EGRET experiment on the Compton GRO can be easily studied. Since the energy threshold of a Cherenkov telescope is inversely proportional to the telescope aperture (until the aperture exceeds the shower diameter!), in principle by increasing the mirror collection area it is technically possible to achieve a threshold of 10 GeV. To achieve this lower threshold, arrays of large, but relatively crude, optical reflectors will be required; these should be located preferably in dark sites on high mountain plateaus with good records of clear skies. At these energies the principal background will be from single muons and cosmic electrons.

The optimum design of these new third-generation telescopes is still a matter of debate and a series of international workshops (in Palaiseau, France in 1992, in Calgary, Canada in 1993 and in Tokyo, Japan in 1994) have been held to consider the various possibilities. The concepts that have been considered include:

(a) Arrays of optical reflectors of 10m aperture; this is a no-risk extension of existing proven imaging techniques and is already been undertaken at the Whipple site in Arizona, U.S.A., at the HEGRA experiment on the Canary Islands, at the Durham experiment in Narrabri, Australia and at the CANGAROO experiment in Woomera, Australia. Although strictly speaking these might be considered advanced second-generation telescopes these facilities can be easily expanded to study energies below 100 GeV. The imaging technique may not be as effective below 100 GeV but other techniques, such as the measurement of the lateral distribution, can be used.

(b) Arrays of "heliostats" focussed to a common detector; these experiments are centered on the use of existing solar power plants where the solar plant is modified to do double duty as an astronomical telescope at night. There are two groups investigating this concept; a U.S. group investigating the use of the operating Solar-1 power plant in Barstow, California and a French group planning to use the defunct solar power plant in Themis, France. These plants are superficially attractive because the mirrors already exist but in practice the optical layout is not ideal, it is not always easy to mesh solar power generation by day and gamma-ray astronomy by night, and the existing locations are not prime astronomical sites.

(c) Large fixed "Arecibo"-type optical dishes; the dish must have an aperture twice the diameter of the shower pool (>200m) since the multi-element cameras only see half the mirrors at any one time. This telescope concept is the most ambitious (with a cost similar to that of a space gamma-ray telescope) but it still lacks a detailed design. A serious limitation is the restricted sky coverage.

It is expected that the next generation of space telescopes e.g. GLAST, AGATE, etc., will extend the useful range of space gamma-ray astronomy into the 10–100 GeV region; given the large estimated cost of these missions (about $100M) it is unlikely that these telescopes will be operational before the end of the century. Large Atmospheric Cherenkov Telescopes of the type discussed above will effectively complement and extend these missions; because they can be built in stages they could be operational before the next generation of space telescopes and could begin to address many of the important scientific issues in the 10–1000 GeV range before the next millennium.

Acknowledgements

The authors thank D. Lewis, R. Ong, H.J. Rose, M. Urban, and A. Weekes for helpful comments on the manuscript. Research in gamma-ray astronomy at the Harvard-Smithsonian Center for Astrophysics is supported by the Department of Energy, and at St. Patrick's College, Maynooth, by FORBAIRT, the Irish scientific funding agency.

References

Aharonian, F.A., *et al.* 1991a, *Proc. 22nd Internat. Cosmic Ray Conf. (Dublin)*, **2**, 615
Aharonian, F.A., *et al.* 1991b, *Nuclear Inst. and Methods, A*, **302**, 522
Akerlof, C.W., *et al.* 1989, *Proc. GRO Science Workshop (Goddard)*, 4-49
Akerlof, C.W., *et al.* 1991, *Astrophys. J.*, **377**, L97
Anassontzis, E., *et al.* 1992, *Nuclear Inst. and Methods, A*, **315**, 267
Baillon, P., *et al.* 1991, *Proc. 22nd Internat. Cosmic Ray Conf. (Dublin)*, **1**, 220
Baillon, P., *et al.* 1993a, *Proc. Workshop on 'Towards a Major Atmospheric Cherenkov Detector — II'*, Ed. R.C. Lamb, p121
Baillon, P., *et al.* 1993b, *Astroparticle Physics*, **1**, 341
Basa, S., *et al.* 1992, *Proc. Workshop on 'Towards a Major Atmospheric Cherenkov Detector '*, Ed. P. Fleury and G. Vacanti, Editions Frontieres, p205
Bowden, C.C.G., *et al.* 1992, *Astroparticle Physics*, **1**, 47
Bowden, C.C.G., *et al.* 1993, *Proc. Workshop on 'Towards a Major Atmospheric Cherenkov Detector — II'*, Ed. R.C. Lamb, p230
Brazier, K.T., *et al.* 1989, *Expt. Astron.*, **1**, 77
Burnett, T.H., *et al.* 1990, *Astrophys. J.*, **349**, L25
Carramiñana, A., *et al.* 1989, *Astrophys. J.*, **346**, 967
Cawley, M.F., *et al.* 1990, *Expt. Astron.*, **1**, 173
Chilingarian, A.A., and Cawley, M.F. 1991, *Proc. 22nd Internat. Cosmic Ray Conf. (Dublin)*, **1**, 460
Chilingarian, A.A., *et al.* 1991, *Proc. 22nd Internat. Cosmic Ray Conf. (Dublin)*, **1**, 480
Chudakov, A.E., *et al.* 1965, *Transl. Consultants Bureau, P.N. Lebedev Phys. Inst.*, **26**, 99
Danaher, S., *et al.* 1993, *Astroparticle Phys.*, **1**, 357
Davies, J.M., and Cotton, E.S. 1957, *J. of Solar Energy*, **1**, 16
de Jager, O.C., *et al.* 1990, *Nucl. Phys. B (Proc. Suppl.*, **14A**, 169
Degrange, B., *et al.* 1993, *Proc. Workshop on 'Towards a Major Atmospheric Cherenkov Detector — II'*, Ed. R.C. Lamb, p235
Delaney, C.F.G., and Finch, E.C. 1992, *'Radiation Detectors'*, Oxford University Press
Dowthwaite, J.C., *et al.* 1984, *Astrophys. J. Lett.*, **286**, L35
Ebisuzaki, S., *et al.* 1991, *Proc. 22nd Internat. Cosmic Ray Conf. (Dublin)*, **2**, 607
Fleury, P. 1993, *Proc. Workshop on 'Towards a Major Atmospheric Cherenkov Detector — II'*, Ed. R.C. Lamb, p188
Goret, P., *et al.* 1993, *Astron. Astrophys.*, **270**, 401
Gorham, P.W. 1986, *Ph.D. Thesis, U. of Hawaii* (unpublished)
Grindlay, J.E. 1972, *Astrophys. J. Lett.*, **174**, L9
Halzen, F., *et al.* 1991, *Proc. 22nd Internat. Cosmic Ray Conf. (Dublin)*, **1**, 504
Hara, T., *et al.* 1993, *Nuclear Inst. and Methods, A*, **332**, 300
Harris, K., *et al.* 1992, *Proc. Workshop on 'Towards a Major Atmospheric Cherenkov Detector '*, Ed. P. Fleury and G. Vacanti, Editions Frontieres, p189
Hillas, A.M. 1985, *Proc. 19th Internat. Cosmic Ray Conf. (La Jolla)*, **3**, 445
Hillas, A.M. 1989, *Proc. Workshop on Very High Energy Gamma-ray Astronomy (Crimea)*, Ed. A.A. Stepanian, D.J. Fegan, and M.F. Cawley, p134
Hillas, A.M., and Patterson, J.R. 1990, *J. Phys. G.*, **16**, 1271
Hillas, A.M., and West, M. 1991, *Proc. 22nd Internat. Cosmic Ray Conf. (Dublin)*, **1**, 472
Jiang, Y., *et al.* 1993,*Proc. 23rd Internat. Cosmic Ray Conf. (Calgary)*, **4**, 662
Kalekin, O.R., *et al.* 1994, *Proc. Workshop on 'Towards a Major Atmospheric Cherenkov Detector — III'*, Ed. T. Kifune, (in press)
Karle, A., *et al.* 1991, *Proc. 22nd Internat. Cosmic Ray Conf. (Dublin)*, **4**, 666
Kifune, T., *et al.* 1993, *Proc. Workshop on 'Towards a Major Atmospheric Cherenkov Detector — II'*, Ed. R.C. Lamb, p39
Kifune, T., *et al.* 1995, preprint
Krys, A., Krys, E., and Wasilewski, A. 1991, *Proc. 22nd Internat. Cosmic Ray Conf. (Dublin)*, **2**, 638
Lang, M.J., 1991, *Ph.D. Thesis, National University of Ireland* (unpublished)

Lewis, D.A. 1990, *Expt. Astron.*, **1**, 213
Lewis, D.A., *et al.* 1991, *Proc. 22nd Internat. Cosmic Ray Conf. (Dublin)*, **1**, 508
Loeffler, F.J. 1993, *Nuclear Inst. and Methods, A*, **332**, 310
Lorenz, E. 1993, *Proc. Workshop on 'Towards a Major Atmospheric Cherenkov Detector — II'*, Ed. R.C. Lamb, p182
MacMinn, D., and Primack, J.R. 1995, preprint
Mattox, J.R. 1988, *Nuclear Inst. and Methods,*, **A,271**, 652
Mirzoyan, R. 1992, *Proc. Workshop on 'Towards a Major Atmospheric Cherenkov Detector'*, Ed. P. Fleury and G. Vacanti, Editions Frontieres, p239
Morse, R., *et al.* 1993, *Proc. Workshop on 'Towards a Major Atmospheric Cherenkov Detector — II'*, Ed. R.C. Lamb, p75
North, A.R., *et al.* 1987, *Nature*, **326**, 567
Ogio, S., *et al.* 1993, *Proc. 23rd Internat. Cosmic Ray Conf. (Calgary)*, **1**, 392
Punch, M., *et al.* 1991, *Proc. 22nd Internat. Cosmic Ray Conf. (Dublin)*, 1, 464
Punch, M., *et al.* 1992, *Nature*, **358**, 477
Raubenheimer, B.C., *et al.* 1993, *Proc. Workshop on 'Towards a Major Atmospheric Cherenkov Detector — II'*, Ed. R.C. Lamb, p87
Reynolds, P.T. 1991, *Proc. 22nd Internat. Cosmic Ray Conf. (Dublin)*, **1**, 496
Reynolds, P.T., *et al.* 1993, *Astrophys. J.*, **404**, 206
Resvanis, L.K., *et al.* 1986, *NATO ASI Series, Very High Energy Gamma Ray Astronomy*, Ed. K.E. Turver, p225
Resvanis, L.K., *et al.* 1988, *Nuclear Inst. and Methods, A*, **269**, 297
Roberts, M.D., *et al.* 1991, *Proc. 22nd Internat. Cosmic Ray Conf. (Dublin)*, **2**, 645
Rowell, G.P., *et al.* 1991, *Proc. 22nd Internat. Cosmic Ray Conf. (Dublin)*, **2**, 642
Salamon, M.H., Stecker, F.W., and de Jager, O.C. 1994, *Astrophys. J.*, **423**, L1
Schubnell, M., *et al.* 1992, AIP Conference Proceedings, **280**, 1171
Sinitsyna, V.G. 1993, *Proc. Workshop on 'Towards a Major Atmospheric Cherenkov Detector — II'*, Ed. R.C. Lamb, p91
Sinnis, G. 1992, *Proc. Workshop on 'Towards a Major Atmospheric Cherenkov Detector '*, Ed. P. Fleury and G. Vacanti, p305
Tilav, S., *et al.* 1993, *Proc. Workshop on 'Towards a Major Atmospheric Cherenkov Detector — II'*, Ed. R.C. Lamb, p72
Stamm, W., Sauerland, K., and Müller, N. 1993, *Nuclear Inst. and Methods, A*, **328**, 601
Tornabene, H.S., and Cusimano, F.J. 1968, *Canad. J. Phys.*, **46**, S581
Tumer, O.T., *et al.* 1990, *Proc. 21st Internat. Cosmic Ray Conf. (Adelaide)*, **2**, 155
Urban, M., *et al.* 1990, *Nucl. Phys. (Proc. Suppl.)*, **14B**, 223
Vacanti, G., *et al.* 1991, *Astrophys. J.*, **377**, 467
Vacanti, G., *et al.* 1994, *Astroparticle Physics*, **2**, 1
Vishwanath, P.R., *et al.* 1993, *Proc. Workshop on 'Towards a Major Atmospheric Cherenkov Detector — II'*, Ed. R.C. Lamb, p115
Vladimirskii, B.M., *et al.* 1989, *Proc. Workshop on VHE Gamma-ray Astronomy (Crimea)*, Eds. A.A. Stepanian, D.F. Fegan, M.F. Cawley, p21.
Weaverdyck, C., Meyer, D., and Akerlof, C. 1991, *Nuclear Inst. and Methods, A*, **310**, 690
Weekes, T.C. 1976, *Nuovo Cimento*, **35B**, 95
Weekes, T.C. 1981, *Proc. 17th Internat. Cosmic Ray Conf. (Paris)*, **8**, 34
Weekes, T.C. 1988, *Phys. Rep.*, **160**, 1
Weekes, T.C., and Turver, K.E. 1977, *Proc. 12th ESLAB Symp. (Frascati)*, **ESA SP-124**, 279
Weekes, T.C., *et al.* 1989, *Astrophys. J.*, **342**, 379